

Fluctuation Studies at the Subnuclear Level of Matter: Evidence for Stability, Stationarity and Scaling *

LIU Qin^{1†} and MENG Ta-chung^{1,2‡}

¹*Department of Physics, CCNU, 430079 Wuhan, China*

²*Institut für Theoretische Physik, FU-Berlin, 14195 Berlin, Germany*

(Dated: May 26, 2020)

It is pointed out that the concepts and methods introduced by Bachelier and by Mandelbrot to Finance and Economics can be used to examine the fluctuations observed in high-energy hadron production processes. Theoretical arguments and experimental evidences are presented which show that the relative variations of hadron-numbers between successive rapidity intervals are non-Gaussian stable random variables, which exhibit stationarity and scaling. The implications of the obtained results are discussed.

PACS numbers: 13.85.Tp, 13.85.Hd, 05.40.-a

I. HADRON-PRODUCTION IN HIGH-ENERGY COLLISIONS

It is a well-known fact that hadrons (for example pions, kaons, protons, neutrons, \dots , and their antiparticles) can be produced in lepton-, hadron- and nucleus- induced reactions at sufficiently high incident energies. In such processes, we are witnessing an impressive demonstration of energy-conversion into matter, where energy-momentum conservation requires that the total (c.m.s.) energy of the colliding system must be high enough to create the masses of the produced hadrons and provide them with sufficient kinetic energies. A vast amount of data exists for such hadron-formation processes where the multiplicity-, transverse-momentum- and rapidity-distributions of the produced hadrons in high-energy hadron-hadron, hadron-nucleus and nucleus-nucleus collisions have been accumulated, and part of them, especially those at extremely high energies are taken from cosmic-ray experi-

* Supported by the National Natural Science Foundation of China under Grant No.70271064.

† Email address: liuq@ccnu.edu.cn

‡ Email address: meng@ccnu.edu.cn; meng@physik.fu-berlin.de

ments.

Much effort has been made to describe these data. The conventional way of doing this is to divide such a hadron-production process, in accordance with the currently most popular picture for subnuclear structure and subnuclear dynamics, conceptually into three steps:

In step I, the incident-hadron (a free hadron or a bounded hadron namely that inside a nucleus) is pictured as a large swarm of partons (quarks, antiquarks and gluons) where everyone of them carries a fraction (known as the Feynman- x and denoted by x_F or simply by x , with x_F or x between zero and unity) of the longitudinal (that is along the incident axis) momentum of this hadron. The distribution of x_F for different kinds of partons (for example: the u, d, s valence quarks, the sea-quark-pairs; or the gluons) has been carefully parameterized; and the corresponding parton distributions can be readily found in the literature [1].

In step II, it is envisaged that some of the partons in the projectile-hadron are scattered by some of the partons in the target-hadron. They interact with one another according to the Feynman rules derived from the given QCD-Lagrangian. Under the assumption that some classes of reaction-mechanisms are more important than the others and the perturbative methods are applicable, one can evaluate the corresponding Feynman graphs. Details of such calculations have been worked out, and can be readily found in the literature [1].

In step III, the observed final-state hadrons are assumed to be directly related to the scattered partons mentioned in Step II. The relations between the scattered partons and the observed hadrons are parameterized in terms of “fragmentation functions”. Fragmentation functions for all possible kinds of partons have been worked out, and they can also be readily found in the literature [1].

In connection with the above-mentioned three-step-approach, it is of considerable importance to recall [1] the following facts: (A) Quarks, antiquarks and gluons have not been, and according to QCD and Confinement they can never be, directly measured. (B) Perturbative methods can be used only when the momentum transfer in the scattering process is so large that the corresponding QCD running coupling constant is less than unity; but the overwhelming majority of such hadron-production processes are soft in the sense that the momentum transfer is relatively low. These facts imply that, it *has not been* possible, and it *can never be* possible, to have an *experimental check* for the three steps *individually*.

In the present paper, we discuss such hadron-production processes from a different view-

point and ask the following questions: Suppose we focus our attention *only* on the directly measurable quantities (such as the rapidity distributions of the produced charged hadrons), and try to perform a preconception-free data-analysis where we rely as much as possible on the relevant knowledge of Mathematical Statistics [such as the Law of Large Numbers and the (Generalized) Central Limit Theorem], shall we be able to extract useful information on the reaction mechanisms of such hadron-production processes by examining the experimental data? If yes, what can we learn from such information? Can such information be used, for example, to make predictions for future experiments, and/or to check the consequences of the conventional approach mentioned above?

Since a considerable part of the available first-hand information on hadron-production processes are distributions of few directly measurable quantities (such as the multiplicity n_{ch} of charged hadrons; the rapidity y or the pseudorapidity η and the transverse momentum p_{\perp} or transverse energy E_{\perp} of such a hadron), concepts and methods in Probability Theory and Mathematical Statistics are expected to play a distinguished role in describing/understanding the existing data, and in making predictions for future experiments.

II. FROM RANDOM WALK TO STABLE DISTRIBUTIONS IN FINANCE AND ECONOMICS

It is well-known that fluctuation studies are of considerable importance in non-equilibrium as well as in equilibrium systems; and there are several reasons for this. One of them is that, deviations for or fluctuations about the mean values are always present, even when the system under consideration is in equilibrium. Another is that fluctuation studies provide a natural framework for understanding a large classes of phenomena, among which the best known phenomenon is “Brownian motion” or “the random walk”—known through Albert Einstein’s work starting 1905 [2].

It is, however, not very well-known (at least not among the particle physicists) that, five years earlier, in 1900, a then young French student named Louis Bachelier has constructed a random walk theory for security and commodity markets [3]. The essence of Bachelier’s theory is the following: Consider the successive differences of two adjacent spot prices

$$L_B(t, T) = z(t + T) - z(t), \quad (1)$$

where $z(t + T)$ and $z(t)$ is the spot price of a stock or that of a piece of commodity at the end of a period of time $t + T$ and t respectively; and assume that the set of all $L_B(t, T)$'s are statistically independent, Gaussian (normally) distributed random variables with zero mean, and variance proportional to the differencing interval T . This assumption is often called [4] the Gaussian hypothesis [3], and the arguments supporting this hypothesis are based on the Central Limit Theorem (cf. Appendix A and the references given therein). To be more precise, if the price changes from transaction to transaction are independent, identically distributed random variables with *finite* variance, and if transactions are *fairly uniformly* spaced through time, the Central Limit Theorem will lead us to believe that price changes across differencing intervals such as a day, a week, or a month should be Gaussian distributed, because they are simple sums of the changes from transaction to transaction. Detailed comparisons between this hypothesis and empirical data have been performed by a number of authors [4]. Despite the fundamental importance of Bachelier's work [3], it has been become obvious that this hypothesis cannot be right as it stands (some details will be given in Section IV). In this sense, Mandelbrot's theory [4, 5, 6] can be understood as an improvement and a generalization of Bachelier's [3].

The main difference between the theory of Bachelier and that of Mandelbrot is the following. Instead of Gaussian (normally distributed) random variables with zero mean and finite (which can be normalized to unity) variance, Mandelbrot made the assertion that the variance of the random variable

$$L_M(t, T) = \ln z(t + T) - \ln z(t) \quad (2)$$

can behave as if it is *infinite*; and consistent with this, he suggested that the Gaussian distribution should be replaced by a rich class of probability distributions called *stable distributions* among which Gaussian is a limiting case with finite variance. It is known (cf. Appendix A and the references given therein) that such distributions allow skewness and heavy tails, and have many intriguing mathematical properties. One of the important properties is that, instead of the above-mentioned Central Limit Theorem, they satisfy the *Generalized* Central Limit Theorem (cf. Appendix A and the references given therein). Above all, evidences have been found that the empirical distributions conform best to the non-Gaussian members of this family of distributions.

It is of considerable importance to keep in mind that the statistical distributions in

Mandelbrot's Fractal Approach to Finance and Economics are *stable*, *stationary*, and *scale-invariant* (in other words, *scaling*). Furthermore, such distributions can have one or several of the following properties. (a) Repeated instances of sharp discontinuity can combine with continuity. (b) Concentration can automatically and unavoidably replace evenness. (c) Non-periodic cycles can automatically and unavoidably follow from long-range dependence. While some of the mathematical aspects of the above-mentioned concepts are summarized in Appendix A, the methods and results of comparing such concepts with experimental data will be discussed in Section IV.

III. RAPIDITY, LOCALITY AND LIGHT-CONE VARIABLES IN HIGH-ENERGY HADRON-PRODUCTION PROCESSES

Quantitative information about the produced hadrons in high-energy collisions exists mostly in form of distributions (histograms) of the measured quantities; and one of the few distributions that can be, and has been, well measured is the rapidity (y) or pseudorapidity (η) distribution of the electrically charged hadrons produced in such processes.

The rapidity of an observed hadron of mass m , energy E , momentum $\vec{p} = (p_{\parallel}, \vec{p}_{\perp})$ where p_{\parallel} and \vec{p}_{\perp} are the momentum in the parallel and that in the transverse direction of the collision axis respectively, is defined as

$$y = \frac{1}{2} \ln\left(\frac{E + p_{\parallel}}{E - p_{\parallel}}\right). \quad (3)$$

This can also be written as $y = \ln[(E + p_{\parallel})/E_{\perp}]$, where $E_{\perp} = M_{\perp} = (m^2 + |\vec{p}_{\perp}|^2)^{1/2}$ is known as the "transverse energy" or "transverse mass". Due to the fact that the overwhelming part of the produced hadrons are energetic pions (the mass of which is negligibly small compared with the average value of p_{\parallel}), and that their transverse momenta are exponentially distributed with relatively small average $|\vec{p}_{\perp}|$, the corresponding pseudorapidity

$$\eta = \frac{1}{2} \ln\left(\frac{p + p_{\parallel}}{p - p_{\parallel}}\right) \quad (4)$$

is often used as a good approximation for the rapidity y ($y \approx \eta$), where E in Eq. (3) is replaced by $p = (p_{\parallel}^2 + |\vec{p}_{\perp}|^2)^{1/2}$. One of the advantages of using η instead of y is that the former can be expressed in terms of the scattering angle θ ($\eta = -\ln \tan \frac{\theta}{2}$), and thus in order to determine η experimentally, one only needs to measure θ . Furthermore, we can also write $y \approx \eta = \ln[(p + p_{\parallel})/|\vec{p}_{\perp}|]$ and treat $|\vec{p}_{\perp}|$ approximately as a constant.

Significant fluctuations have been observed in rapidity-distributions in hadron-production processes at cosmic-ray [7], and at accelerator energies [8, 9]. The question we raise here is whether such fluctuations can be directly used to gain information on the reaction mechanisms of the above-mentioned processes in general, and information on the space-time properties of such reactions in particular. In order to study such properties, it is useful to keep in mind that the overwhelming part of the produced hadrons are energetic pions which implies that their locations in space-time are mainly concentrated near the light-cone. Hence it is not only meaningful, but also useful to discuss the space-time properties of these hadrons in terms of light-cone variables [10] (and/or quantities directly related to them)

$$x_{\pm} = \frac{1}{\sqrt{2}}(t \pm x_{\parallel}), \quad (5)$$

$$p_{\pm} = \frac{1}{\sqrt{2}}(E \pm p_{\parallel}), \quad (6)$$

where $(t, x_{\parallel}, \vec{x}_{\perp})$ and $(E, p_{\parallel}, \vec{p}_{\perp})$ are canonical conjugates to each other with the property that their 4-product can be written as

$$tE - x_{\parallel}p_{\parallel} - \vec{x}_{\perp} \cdot \vec{p}_{\perp} = x_{-}p_{+} + x_{+}p_{-} - \vec{x}_{\perp} \cdot \vec{p}_{\perp}. \quad (7)$$

Here, we introduce in analogy to rapidity y defined by Eq. (3), a quantity

$$l = \frac{1}{2} \ln\left(\frac{t - x_{\parallel}}{t + x_{\parallel}}\right) \quad (8)$$

which we call locality. This quantity can, again in analogy to y , also be written as $l = \ln[(t - x_{\parallel})/s_{\perp}]$ where $s_{\perp} = (t^2 - x_{\parallel}^2)^{1/2}$ stands for the “transverse interval” whereby $s^2 = t^2 - x_{\parallel}^2 - |\vec{x}_{\perp}|^2$ is the square of the space-time “interval” between the world-point x and the origin $(0, 0, \vec{0})$. Furthermore, we can also define a corresponding “pseudolocality”

$$\lambda = \frac{1}{2} \ln\left(\frac{r - x_{\parallel}}{r + x_{\parallel}}\right), \quad (9)$$

where r in $s^2 = t^2 - r^2$ stands for $r = (x_{\parallel}^2 + |\vec{x}_{\perp}|^2)^{1/2}$. While the dynamics of a system can be described either in terms of space-time variables or in terms of their canonical conjugates, it is certainly of considerable interest to have a physical picture in space-time.

Dealing with subnuclear phenomena, it is clear that we need to take care of the commutation relations [11] between quantities which are canonical conjugates to each other. From

$[E, t] = i$ and $[p_{\parallel}, x_{\parallel}] = -i$, we readily obtain the corresponding commutation relations not only between the light-cone variables x_{\pm} and p_{\pm} , but also those between l and y as well as those between λ and η . While the derivation and the explicit expressions of these relations are not very interesting, one of the consequences should be mentioned: By using a very general form of W. Heisenberg's uncertainty principle developed in 1929 by H. P. Robertson [12], the following can be obtained. If we are interested in the simultaneous specification of two observables A and B , the corresponding operators of which obey a non-zero commutation relation $[A, B] = iC$ (i is included for convenience; for $A = x_{\parallel}$ and $B = p_{\parallel}$ we have $C = \hbar$), and if we consider a state $|\psi\rangle$ which is normalized but otherwise arbitrary (i.e. not necessarily eigenstate of either A or B), then, the root mean square derivations of A and B as the square-roots of the corresponding quantities satisfy $\Delta A \Delta B \geq \frac{1}{2} |\langle C \rangle| = \frac{1}{2} |\langle [A, B] \rangle|$, which is an exact and precise form of the uncertainty principle. Note that, no matter whether C in the commutation relation is an operator or simply a constant, the right-hand side of the above equation is always a constant. By applying this to y and l or directly to η and λ , we obtain

$$\Delta \eta \Delta \lambda \sim K, \quad (10)$$

where K is a constant (which is independent of the choice of Lorentz-frames). As we shall see in Section IV, the uncertainty principle and its immediate consequences indeed play an important role in interpreting the obtained results.

IV. PROBING STABILITY, STATIONARITY AND SCALING

As far as the idea and the mathematical basis are concerned, both Bachelier's Gaussian hypothesis [3] and Mandelbrot's hypothesis [4, 5, 6] have to be considered as master-strokes, yet what really counts is whether the relevant hypothesis indeed describes the empirical data. In this connection, it has been observed that the Gaussian hypothesis [3] can, for example, neither explain the typical erratic behavior of the empirical sample second moments, nor reproduce the extremely heavy tails of the empirical distributions. On the other hand, Mandelbrot's fractal approach to Finance and Economics [4, 5, 6] is well supported by empirical facts. This conclusion is reached after a series of detailed comparisons between empirical data and the characteristic features of the Mandelbrot's theory, namely (A) stability (B) stationarity and (C) scaling, has been performed [4, 5, 6].

Taken together with the facts mentioned in Section III, these comparisons have led us to the following question: Can the concepts and methods introduced to Finance and Economics by Bachelier and by Mandelbrot be helpful in studying and understanding fluctuations in subnuclear reactions?

We recall that pseudorapidity η (or rapidity y) is a continuous variable, and that the multiplicity $dN/d\eta(\eta)$ of charged hadrons at any η (within the allowed kinematical range $\eta_{min} \leq \eta \leq \eta_{max}$) can be very well measured. Hence it is not only meaningful but also possible to consider for a given event the multiplicity as well as its relative changes in an interval $\Delta\eta$ of any size [for details, see below especially item (d)] in the allowed kinematical range. Based on the facts mentioned above, it seems tempting to introduce, by analogy to Mandelbrot's $L_M(t, T)$ shown in Eq. (2), the quantity:

$$L(\eta, \Delta\eta) = \ln \frac{dN}{d\eta}(\eta + \Delta\eta) - \ln \frac{dN}{d\eta}(\eta), \quad (11)$$

and to examine its properties. What we see, as far as the kinematical limits and the experimental resolution allow, are the following. (a) The $L(\eta, \Delta\eta)$'s can be *any* real number. (b) The $L(\eta, \Delta\eta)$'s are summable, in the sense that the adjacent η -interval can be combined or divided in an arbitrary manner without having any influence on the definition of $L(\eta, \Delta\eta)$ given in Eq. (11). (c) The set of $L(\eta, \Delta\eta)$'s can be viewed as approximately statistically independent, identically distributed random variables. It follows then from the *Generalized* Central Limit Theorem (cf. Appendix A and the references given therein) that the only possible class of limiting distributions should be *stable distributions*, which reduce to the special case Gaussian if the $L(\eta, \Delta\eta)$'s have not only a mean, but also a finite variance. (d) Since discontinuities are allowed to occur in Mandelbrot's theory, the bin-size can be chosen to be so small that even $dN/d\eta=0$ can be included. It should be pointed out, however, that $dN/d\eta = 0$ does not occur in the JACEE-data as long as the bin-size is not chosen to be smaller than $\Delta\eta = 0.1$ which stands for the resolution power of these experiments. (e) The variables η and $\Delta\eta$ in $L(\eta, \Delta\eta)$ are, in contrast to t and $T \equiv \Delta t$ in Bachelier's $L_B(t, T)$ and Mandelbrot's $L_M(t, T)$, *not* part of space-time, but as we have mentioned in Section III, the dynamics of the system of produced hadrons should *not* depend on whether we choose space-time or their canonical conjugates as independent variables.

In the second part of this section, we perform a detailed comparison between our theoretical expectations and the available data, and show that the empirical distributions obtained

from the relevant experimental data are not only *stable* but also *non-Gaussian*. Furthermore, we present evidence for *stationarity* and *scale-invariance (scaling)*.

We consider the cosmic-ray data obtained by JACEE-Collaboration [7] for Si+AgBr at 4 *TeV/nucleon* and those for Ca+C (or O) at 100 *TeV/nucleon*. These data have attracted much attention not only because they show results of hadron-production processes in nucleus-nucleus collisions obtained at energies much higher than those obtained from accelerator-experiments, but also because they exhibit unusually high multiplicities as well as significant fluctuations in rapidity-distributions measured in more than 8 to 10 units of η . Among the theoretical discussions on these two single-events [7], the work by Takagi [13] and that by Bialas and Peschanski [14] are the most well-known ones. In fact, their [13, 14] two-component conjecture for single-event rapidity-distributions, in particular for those published by JACEE-Collaboration [7] has been adopted by most physicists working in this field. According to their [13, 14] conjecture, the observed rapidity-distribution of a given event can be, and should be, viewed as a superposition of two distinct parts, namely a “statistical” part and a “nonstatistical” or “dynamical” part. In Takagi’s paper [13], the “statistical” part is described “by a smooth function with least oscillation” where he “assume(s) rather arbitrarily a function of the form \dots ”. According to Bialas and Peschanski [14], the “statistical” part of such single-event distributions should be determined as follows: “If the inclusive rapidity spectrum (averaged over many events) are not available as e.g. when one considers a single high-multiplicity event, it is necessary to invoke one’s theoretical prejudices on the shape of the inclusive spectrum in order to draw definite conclusions.”

In order to study the “nonstatistical” or “dynamical” part, Takagi [13] suggested that “the rapidity density fluctuation of nonstatistical origin may manifest itself as an oscillatory pattern \dots ”. In his paper, the fluctuations are analyzed by use of power spectrum. To study this part, Bialas and Peschanski [14] propose “to study the dependence of factorial moments of the rapidity distribution on the size of the resolution” “by adapting the well-known results obtained in the investigation of cascading phenomena and turbulent behavior”. Based on the above-mentioned two-component conjecture [13, 14], the random cascading model [14] and the method of factorial moments [14], a large amount of experimental data has been analyzed, and many refined models (including scaling models, multifractal models etc.) have been developed. An overview of this development together with the obtained results as well as detailed references can be found in the review article by De Wolf, Dremin and Kittel [9].

“Understanding” fluctuations in empirical data by conjecturing that the measured distribution of a given event consists of two or more components (where every component fulfills its designed goal) has also been rather popular in Finance and Economics, especially in the pre-Mandelbrot era. Based on such a conjecture, many models have been developed and very good fits to the data have been produced. But, according to Mandelbrot [5]: “A common feature of all these approaches, however, is that each new fact necessitates an addition to the explanation. Since a new set of parameters is thereby added, I don’t doubt that reasonable curve-fitting is achievable in many cases. ” In fact he clearly expresses his doubts about the usefulness of such approach in following terms [4, 5]. “This form of symptomatic medicine (a new drug for each complaint) could not be the last word!” “In my view, even if an accumulation of quick fixes were to yield an adequately fitting patchwork, it would bring no understanding.”

We begin our preconception-free data-analysis by noting that the experimental resolution in the given histogram is 0.1, and by choosing this to be the smallest η -interval, $\Delta\eta$. In doing so, the η -range of the Si+AgBr event (hereafter referred to as JACEE1) from $\eta = -4.0$ to 4.0 is divided into 80 $\Delta\eta$ -bins, which lead to a set of 79 $L(\eta, \Delta\eta)$ ’s. Similarly, the η -range of the Ca+C (or that of Ca+O) event (hereafter referred to as JACEE2) from -5.0 to 5.0 is divided into 100 $\Delta\eta$ -bins; hence there are 99 $L(\eta, \Delta\eta)$ ’s. In order to probe whether these experimental values for $L(\eta, \Delta\eta)$ ’s can indeed be considered as *stable* random variables which satisfy the *Generalized* Central Limit Theorem, we make use of the definitions and theorems summarized in Appendix A. To be more precise, we check this in three steps.

In Step (i), we calculate the “running sample mean” of the $L(\eta, \Delta\eta)$ ’s

$$\bar{L}_n(\Delta\eta) = \frac{1}{n} \sum_{i=1}^n L(\eta_i, \Delta\eta). \quad (12)$$

Here, n stands for the ordering number of the $\Delta\eta$ -bins where $\eta_i = \eta_{min} + (i - 1)\Delta\eta$ and the ordering begins from $\eta = \eta_{min}$ which is -4.0 for JACEE1, and -5.0 for JACEE2 respectively. The results are shown in Fig. 1 and Fig. 2 respectively. They seem to have the tendency of approaching zero for sufficiently large n in accordance with the Law of Large Numbers (cf. Appendix A).

In Step (ii), we divide each one of the two $L(\eta, \Delta\eta)$ -sets (JACEE1 and JACEE2) into two distinct groups according to the sign of every individual $L(\eta, \Delta\eta)$, and plot separately, in accordance with Definition A.2 given in Appendix A, the right- and the left-tail distributions

$P(L > L^+)$ and $P(L < L^-)$ respectively. The result for JACEE1 is shown in Fig. 3, and that for JACEE2 is shown in Fig. 4. The purpose of performing the plots are twofold: First, we can see whether the distribution exhibits left-right symmetry and thus determine the skewness parameter β in case the distribution is indeed stable (cf. Theorem A.3 in Appendix A). Second, we can use them as the basis for a detailed stability-test. See Figs. 5 and 6 for details.

In Step (iii), we start with the definition of stability

$$S_m \stackrel{d}{=} c_m L + \gamma_m \quad (13)$$

and note that in accordance with Definition A.1 and Theorem A.1, the necessary and sufficient condition for the $L(\eta, \Delta\eta)$'s to be *stable* random variables is that for all integers $m > 1$, there exist constants $c_m > 0$ and γ_m such that Eq. (13) is true, where

$$\begin{aligned} S_m &= \sum_{i=1}^m L(\eta_i, \Delta\eta) \\ &= L(\eta, m\Delta\eta) \\ &= \ln \frac{dN}{d\eta}(\eta + m\Delta\eta) - \ln \frac{dN}{d\eta}(\eta) \end{aligned}$$

and the $L(\eta_i, \Delta\eta)$'s are identical copies of $L(\eta, \Delta\eta)$ and $c_m = m^{1/\alpha}$ with $0 < \alpha \leq 2$ and γ_m is an arbitrary real number. In order to probe the validity of Eq. (13), we choose the distributions mentioned in “ $\stackrel{d}{=}$ ” to be tail distributions. As the first step, we calculate and plot the right-hand-side of

$$c_m^{-1}(S_m - \gamma_m) \stackrel{d}{=} L \quad (14)$$

for the sets of $L(\eta, \Delta\eta)$'s obtained from JACEE1 and that of JACEE2 respectively (they are of course the same as those shown in Fig. 3 and Fig. 4. The purpose of reproducing them here will become clear below). Next, we set m on the left-hand-side of Eq. (14) to be 2, 3, 4, 5 and 6 which corresponds to the η -interval $m\Delta\eta$ respectively (that is m times 0.1), and determine in every case the most suitable c_m and γ_m ($m=2, 3, 4, 5$ and 6). We then use the method described in Step (ii) to calculate the corresponding $c_m^{-1}(S_m - \gamma_m)^+$'s and $c_m^{-1}(S_m - \gamma_m)^-$'s and plot for every m its right-tail distribution $P(c_m^{-1}[S_m - \gamma_m] > c_m^{-1}[S_m - \gamma_m]^+)$, and its left-tail distribution $P(c_m^{-1}[S_m - \gamma_m] < c_m^{-1}[S_m - \gamma_m]^-)$. It turns out that in these two JACEE-events the maximum of m is $m = 6$, because, beyond this, the sample size would not be large enough to have reasonable statistics. Finally, we compare

the results obtained through the procedure mentioned above in the same figure (here we see why we need the $m = 1$ case in the same scale). The results for JACEE1 are shown in Fig. 5, and those for JACEE2 are shown in Fig. 6. The striking agreement between the distributions of the two sides of Eq. (14) shows that the distributions of random variable $L(\eta, \Delta\eta)$'s under consideration are *indeed* stable distributions.

It should be pointed out that, with the help of the mathematical tools quoted in Appendix A, further information about these stable distributions can be drawn from the results shown in Figs. 1-4: In particular, in accordance with the Law of Large Numbers, Figs. 1 and 2 strongly suggest the existence of zero mean for JACEE1 and JACEE2. Hence it seems meaningful to check, whether the corresponding distributions are symmetric with respect to the mean value and thus determine the skewness parameter β . The fact that the right-tail distributions and the left-tail distributions are approximately equal as we can explicitly see in Figs. 3 and 4, that is $P(L > L^+) = P(L < L^-)$ for JACEE1 and for JACEE2 respectively, shows that $\beta = 0$ in both cases.

Next, we probe stationarity, that is, try to find out whether the sets of $L(\eta, \Delta\eta)$'s obtained from the η -distributions measured at different times (or time-intervals) have *the same* statistical properties. Since we do not have many sets of η -distribution data available, what we *can* do *at present* is only to compare the set obtained from JACEE1 with that obtained from JACEE2. In Fig. 7, $P(L > L^+)$ and $P(L < L^-)$ for these two events are plotted together in the same scale. What we see is that, both the right- and left-tail distributions obtained from JACEE1 are very much the same as those obtained from JACEE2—in agreement with the theoretical expectations. The fact that these two events occurred at different times and in reactions at different energies by using different projectiles and targets makes the observed similarity particularly striking!

Due to the role played by the concept of *scale-invariance* (*scaling*) in the fractal approach to Finance and Economics and its role played in other Sciences including e.g. Condensed Matter Physics, it is quite natural to ask: Are there also empirical evidences, or at least indications, for *scaling* in subnuclear reactions?

One way of checking this is to recall and to apply the method proposed by Mandelbrot [6] in analyzing the spot prices of cotton. He performed such tests in two steps:

In Step 1, he considers the second moment of the daily change of $\ln z(t)$ with $z(t)$ the spot price. Dividing the period under consideration into 30 successive fifty-day samples

which can be numbered in chronological order m , he calculates the second moment of every sample, and plot them against m (cf. Fig. 1 of Ref. [6]). Here, he sees enormous variability in time of the sample second moment, and no tendency of any limiting behavior.

In Step 2, he evaluates the cumulated absolute-frequency distribution by making use of the above-mentioned figure and plot the result on a double logarithmic paper (cf. Fig. 2 of Ref. [6]) in order to check whether the obtained points approximately lie on one straight line. This is because, mathematically, any quantity N that can be expressed as some power of another quantity s , $N(s) = s^{-\tau}$, has the following property. By taking the logarithm on both sides, this equation yields $\ln N(s) = -\tau \ln s$. Hence the scale invariance can be seen from the simple fact that the straight line looks the same everywhere. there are no features at some scale which make that particular scale stand out; that is, as $\ln s$ varies, $\ln N$ shows no kinks or bumps anywhere. What he sees (in Fig. 2 of Ref [6]) is indeed a straight line!

Following Mandelbrot's method, we divide the η -range in JACEE1 and that in JACEE2 into successive 20-bin equal size samples and give everyone of these samples an ordering number m . Due to the fact that, the mean-values of large samples tend to zero (see Fig. 1 and Fig. 2), the second moment (which corresponds to that shown in Fig. 1 of Mandelbrot's paper [6]) is approximately equal to

$$S_{20}^2(\Delta\eta) = \frac{1}{20} \sum_{i=1}^{20} [L(\eta_i, \Delta\eta) - \bar{L}_{20}(\Delta\eta)]^2 \quad (15)$$

which stands for the variance in these two cases. We plot the variance obtained from JACEE1 in Fig. 8, and that from JACEE2 in Fig. 9. As we can explicitly see, their behavior are indeed rather erratic. The corresponding frequency distributions

$$P(S_{20}^2 > s_{20}^2)$$

are plotted in Figs. 10 and 11 respectively. It seems that, in both cases the data indicate the existence of power-law behavior and thus *scale-invariance (scaling)*. It should be pointed out, however, since the number of data points in the JACEE-events are much less than those for cotton-prices in Mandelbrot's analyses, not only the sample-size in our case have to be smaller, but also that the statistics are not as good as those for cotton-prices. In order to amend this deficiency, we propose to use the following alternative method.

Let us consider (instead of the sample variance given in Fig. 1 of Ref. [6], and those used

in Figs. 8 and 9 in this paper) the “running sample variance”

$$S_n^2(\Delta\eta) = \frac{1}{n-1} \sum_{i=1}^n [L(\eta_i, \Delta\eta) - \bar{L}_n(\Delta\eta)]^2, \quad (16)$$

where $\bar{L}_n(\Delta\eta)$ stands for the “running sample mean” shown in Eq. (12) and Figs. 1 and 2. The range of the ordering number n is $n = 2, 3, \dots, 79$ for JACEE1, and $n = 2, 3, \dots, 99$ for JACEE2. The “running sample variance” as a function of the ordering number n is shown in Fig. 12 and Fig. 13. Also in these figures, we see that the sequential sample moment changes rather *erratically* with respect to n , and does *not* seem to tend to any limit. That is to say, erraticity and non-existence of tendency are nevertheless characteristic properties of the plot, although running samples are in general less independent than those obtained by dividing the original set into parts (as it is for example the case in Fig.1 of Ref. [6] and in Figs. 8 and 9 of this paper). In order to see explicitly that running samples do not have much influence on the characteristic features of the original set, we also consider in the JACEE1 case a set of 79 (and similarly in the JACEE2 case a set of 99) Gaussian random variables with zero population mean and unit population variance; and we examine in particular the “running sample variance” of the set of 79 (and the set of 99) Gaussian random variables. What we see (not shown in this paper) is of course distinct differences between the behavior of Gaussian random variables and the that of JACEE-data [7]. A more effective way to examine the scaling behavior of such sets of random variables is to plot the frequency distributions

$$P(S_n^2 > s_n^2)$$

on log – log papers. Such plots for the JACEE-data [7] are shown in Fig. 14 and Fig. 15 respectively. The 78 points obtained from JACEE1 and the 98 points obtained from JACEE2 indeed lie approximately on straight lines in the log – log plots. Having the well-known relationship between scaling, power-law behavior and straight-lines on double logarithmic papers in mind, the straight-line structure in the log – log plots and thus the property of *scale-invariance* (*scaling*) is evident. In order to see whether (and how much if yes) the JACEE-data differ from Gaussian random variables, we also use the above-mentioned sets of 79 and 99 Gaussian random variables to do the same kind of plots, and show them in the corresponding figure, that is in Fig. 14 and Fig. 15 respectively. For such variables, the existence of a scale, namely $\sigma^2 = 1$ (recall that we are considering Gaussian random

variables with zero population mean and unit population variance) can be clearly seen [cf. Eqs. (A14) and (A15) in the appendix].

A number of conclusions can be drawn from the empirical results plotted in Figs. 14 and 15, where once again use have been made of the mathematical tools mentioned in Appendix A. First of all, the result obtained from such log – log plots has to be considered as an effective indicator for scale-invariance (scaling): This is because, in accordance with the Law of Large Numbers for sample variance (see Theorem A.6 in the appendix), there is a profound difference between sets of random variables with finite population variance and those *without* finite population variance. While in the former case, the running sample variance S_n^2 should tend to the population variance σ^2 [see Eqs. (A14)] for large n which plays the role of a scale, there is *no* such limiting behavior in the latter case. The empirical fact that the frequency distributions of S_n^2 obtained from JACEE1 and JACEE2 exhibit power-law behavior shows that the sets of $L(\eta, \Delta\eta)$'s obtained from JACEE1 and JACEE2 *do not have any given scale*. It can be readily seen from the corresponding log – log plots in which the data-points of each JACEE-event lie on a straight line. This behavior is in sharp contrast to that of a sample of Gaussian random variables of the same size. Taken together with Definition A.4, A.5 and Theorem A.4, A.6, the above-mentioned observation shows that the population variance of the JACEE-sets should be infinite and that the originally allowed range for the characteristic exponent α namely $0 < \alpha \leq 2$ should be narrowed down to $0 < \alpha < 2$. In other words, the set of $L(\eta, \Delta\eta)$'s obtained from JACEE1 and those obtained from JACEE2 are indeed *non-Gaussian* stable random variables.

Furthermore, the results of stability tests shown in Figs. 5 and 6 can be, and should also be, considered as evidence for scale invariance (scaling), because also they show that the relevant scale—here the size of η -intervals—does not play a role.

In summary, what we have seen in the second part of this section is that, the analysis of cosmic-ray data shows that the $L(\eta, \Delta\eta)$'s defined in Eq. (11) which are the relative changes of the multiplicities of charged hadrons between successive rapidity-intervals $\Delta\eta$ can be considered as mutually independent random variables, satisfying a *non-Gaussian stable distribution which is stationary and scale-invariant (scaling)*. The striking similarity between the properties of Mandelbrot's $L_M(t, T)$ and those of $L(\eta, \Delta\eta)$ introduced in this paper suggests that the underlying reaction mechanism(s) of the fluctuations in Financial markets and those at the subnuclear level of matter are *very much the same*. To be more specific, we

note that everyone of the $\Delta\eta$'s in $L(\eta, \Delta\eta)$ is related to its corresponding $\Delta\lambda$ through Eq. (10), and the properties of the $L(\eta, K/\Delta\lambda)$'s can be readily expressed in terms of the $\Delta\lambda$'s. In particular, since $\Delta\lambda$ decreases with increasing $\Delta\eta$, measurements within larger and larger values of $\Delta\eta$ correspond to measurements within smaller and smaller values of $\Delta\lambda$. It means, in this context, the validity of stability, stationarity and scaling within larger and larger $\Delta\eta$ intervals implies the validity of such characteristics at smaller and smaller values of $\Delta\lambda$ (intervals in pseudolocality near the light-cone in space-time). Having in mind that stability, stationarity and scaling are *the* fundamental characteristics of Mandelbrot's fractal approach to Finance, the result of the present empirical analysis should perhaps be considered as an indication that *concepts and methods used in Nonlinear Dynamics and/or in Complex Sciences should be helpful in describing/understanding such hadronization processes*. Studies along this line are now underway; the results will be reported elsewhere.

V. CONCLUDING REMARKS

The result obtained from analyzing the cosmic-ray data for hadron-production, by using the concepts and methods introduced by Bachelier and by Mandelbrot to Finance and Economics, shows that it is not only possible but also useful to extract information on subnuclear reactions directly from empirical distributions of measurable quantities. It shows in particular that the fluctuations in rapidity-distributions in the cosmic-ray data have much in common with the fluctuations observed in stock market. The striking similarity seems to suggest that they are complex phenomena of *the same (fractal) nature*. The fact that *non-Gaussian stable distributions which are stationary and scale-invariant (scaling)* describe the existing data remarkably well calls for further attention. It would be very helpful to have comparison with data taken at other energies and/or for other collision processes.

Acknowledgments

The authors thank Cai Xu, Feng Youceng, Hwa Rudolf, Kittel Wolfram, Li Wei, Liang Zuotang, Peng Hong'an, Qian Wanyan, Ratti Sergio P., Sa Benhao, Schertzer Daniel, Yang Chunbin and Zhu Wei for helpful discussions and valuable comments. They also thank National Natural Science Foundation of China and KeYanChu of CCNU for financial suport.

APPENDIX A

This is a mathematical appendix added to the present paper to make it self-contained. It contains a brief introduction to *stable distributions* and a set of definitions and theorems (without proofs) taken from monographs and/or textbooks related to this subject [15].

The term “stable distributions” stands for a rich class of probability distributions which allow skewness and heavy tails, and have a number of other intriguing properties. One of them is the lack of closed formulas for densities and distributions for all but a few; such exceptional stable distributions are Gaussian, Cauchy and Lévy distributions.

Definition A.1 Let X_1, X_2, \dots, X_n and X be mutually independent random variables with a common distribution P which is not concentrated at one point, where $n > 1$ and S_n is the sum of these n random variables $S_n = X_1 + X_2 + \dots + X_n$. Then, the distribution P is *stable in the broad sense* if and only if for each n , there exist constants $c_n > 0$ and γ_n such that

$$S_n \stackrel{d}{=} c_n X + \gamma_n. \quad (\text{A1})$$

Here, the symbol “ $\stackrel{d}{=}$ ” means equality in distribution, i.e. both expressions obey the same probability law. The distribution P is *stable in the strict sense* if and only if $\gamma_n = 0$ for all n .

Theorem A.1 The norming constants c_n are of the form $c_n = n^{1/\alpha}$ with $0 < \alpha \leq 2$, where the constant α is called the characteristic exponent of P .

Theorem A.2 A random variable X is stable if and only if $X \stackrel{d}{=} AZ + B$, where $0 < \alpha \leq 2$, $-1 \leq \beta \leq 1$, $A > 0$, $B \in \Re$ and Z is a random variable with characteristic function

$$E \exp(iuZ) = \exp(-|u|^\alpha [1 - i\beta \tan \frac{\pi\alpha}{2}(\text{sign}u)]) \quad \alpha \neq 1 \quad (\text{A2})$$

$$E \exp(iuZ) = \exp(-|u| [1 + i\beta \frac{2}{\pi}(\text{sign}u) \ln |u|]) \quad \alpha = 1. \quad (\text{A3})$$

Theorem A.3 A general stable distribution requires four parameters to describe. The commonly used set is $\{\alpha, \beta, \gamma, \delta\}$. Here $0 < \alpha \leq 2$ is known as the index of stability or the characteristic exponent; $-1 \leq \beta \leq 1$ the skewness parameter; $\gamma > 0$ the scale parameter; and $\delta \in \Re$ the location parameter. The three exceptional distributions mentioned at the beginning of the appendix, namely

(a) Normal or Gaussian distribution, $X \sim N(\mu, \sigma^2)$ with a density

$$f(x) = \frac{1}{\sqrt{2\pi}\sigma} \exp\left(-\frac{(x-\mu)^2}{2\sigma^2}\right), \quad -\infty < x < \infty, \quad (\text{A4})$$

(b) Cauchy distribution, $X \sim Cauchy(\gamma, \delta)$ with a density

$$f(x) = \frac{1}{\pi} \frac{\gamma}{\gamma^2 + (x-\delta)^2}, \quad -\infty < x < \infty, \quad (\text{A5})$$

(c) Lévy distribution, $X \sim Lévy(\gamma, \delta)$ with a density

$$f(x) = \sqrt{\frac{\gamma}{2\pi}} \frac{1}{(x-\delta)^{3/2}} \exp\left(-\frac{\gamma}{2(x-\delta)}\right), \quad \delta < x < \infty, \quad (\text{A6})$$

are special cases of stable distributions. Also their characteristic functions have precisely the form given in Eqs. (A2) or (A3) mentioned in Theorem A.2. The parameters have respectively the following set of values:

$$X \sim N(\mu, \sigma^2) : \alpha = 2, \beta = 0, A = \sigma^2/2, B = \mu;$$

$$X \sim Cauchy(\gamma, \delta) : \alpha = 1, \beta = 0, A = \gamma, B = \delta;$$

$$X \sim Lévy(\gamma, \delta) : \alpha = 1/2, \beta = 1, A = \gamma, B = \delta.$$

Definition A.2 Let X be a random variable with distribution $P(x)$. Then its *right-tail distribution* $T_r(x)$ is

$$T_r(x) = 1 - P(x) = P(X > x) \quad (\text{A7})$$

where $x \in \Re$ is any real number. The corresponding *left-tail distribution* $T_l(x)$ is

$$T_l(x) = P(x) = P(X < x). \quad (\text{A8})$$

Definition A.3 A distribution is said to be *heavy tailed* if its tails are heavier than exponential. For $\alpha < 2$, stable distributions have one tail (when $\alpha < 1$ and $\beta = \pm 1$) or both tails (all other cases) that are asymptotically power laws with heavy tails.

Definition A.4 Let $f(x)$ be the density function of a stable distribution. The expression

$$E(|X|^p) = \int_{-\infty}^{\infty} dx |x|^p f(x) \quad (\text{A9})$$

is called the fractional absolute moment of this distribution, where p can be any real number.

Theorem A.4 The fractional absolute moment $E(|X|^p)$ is finite if and only if $0 < p < \alpha$ where α is the characteristic exponent of this stable distribution (which satisfies $0 < \alpha < 2$), and that $E(|X|)^p$ is *infinite* for $p \geq \alpha$.

Theorem A.5 Khinchine's Law of Large Numbers

Let $\{X_i(i = 1, 2, \dots, n)\}$ be a sequence of mutually independent random variables with a common distribution. If the expectation $\mu = E(X_i)$ exists, then for every $\varepsilon > 0$, the probability

$$P\left\{\left|\frac{X_1 + X_2 + \dots + X_n}{n} - \mu\right| > \varepsilon\right\} \rightarrow 0 \quad \text{for } n \rightarrow \infty. \quad (\text{A10})$$

It means in the language of Mathematical Statistics: As n tends to infinity, the expression $\frac{1}{n} \sum_{i=1}^n X_i$ converges in probability to μ ; and this is often written as:

$$\frac{1}{n} \sum_{i=1}^n X_i \xrightarrow{P} \mu \quad \text{for } n \rightarrow \infty. \quad (\text{A11})$$

Definition A.5 Let $\{X_i(i = 1, 2, \dots, n)\}$ be a sample of size n taken from the population of a random variable X with population mean $E(X) = \mu < \infty$ and population variance $D(X) = \sigma^2 < \infty$. Then, the expression

$$\bar{X}_n = \frac{1}{n} \sum_{i=1}^n X_i, \quad (\text{A12})$$

which is nothing else but the expression on the left-hand-side of the arrow in (A11), and

$$S_n^2 = \frac{1}{n-1} \sum_{i=1}^n (X_i - \bar{X}_n)^2 \quad (\text{A13})$$

are called, respectively, the "running sample mean" and the "running sample variance" of X .

Theorem A.6 Law of Large Numbers for sample variance

The sample variance S_n^2 defined in Eq. (A13) with \bar{X}_n given by (A12) behaves, for increasing n , as follows:

$$S_n^2 \xrightarrow{P} \sigma^2 \quad \text{for } n \rightarrow \infty, \quad (\text{A14})$$

and for all intergers n , we have:

$$E(S_n^2) = \sigma^2. \quad (\text{A15})$$

Theorem A.7 Central Limit Theorem

Let $\{X_i(i = 1, 2, \dots, n)\}$ be a sequence of mutually independent random variables with a common distribution. If the expectation $\mu = E(X_i)$ and the variance $\sigma^2 = Var(X_i)$ exist, then the sum $S_n = X_1 + X_2 + \dots + X_n$ has the following limiting behavior. For every fixed x ,

$$\lim_{n \rightarrow \infty} P\left\{\frac{S_n - n\mu}{\sigma\sqrt{n}} < x\right\} = \frac{1}{\sqrt{2\pi}} \int_{-\infty}^x dt \exp\left(-\frac{t^2}{2}\right). \quad (\text{A16})$$

This theorem is a special case of the following theorem.

Theorem A.8 Generalized Central Limit Theorem

Let $\{X_i(i = 1, 2, \dots, n)\}$ be a sequence of mutually independent, identically distributed random variables. Then, there exist constants $a_n > 0$, $b_n \in \Re$ and a non-degenerated random variable Z with

$$a_n(X_1 + X_2 + \dots + X_n) - b_n \xrightarrow{d} Z \quad (\text{A17})$$

if and only if Z is stable; in which case $a_n = n^{-1/\alpha}$ for $0 < \alpha \leq 2$.

-
- [1] The theoretical scheme of such an approach can be found in textbooks. See e.g. F. Halzen and A. D. Martin, *Quarks and Leptons: An Introductory Course in Modern Particle Physics* (John Wiley & Sons, New York, Chichester, Brisbane, Toronto, Singapore, 1984); and the references given therein.

The most recent parameterizations can be found by tracing through the review talks given at the relevant international conferences on High Energy Physics and those on Heavy Ion Physics.

- [2] A. Einstein, *Ann. d. Phys.*, **17**, p. 549, 1905. An English translation of his papers on this subject can e.g. be found in: A. Einstein (edited by R. Fürth and translated by A. D. Cowper), *Investigations on the Theory of the Brownian Movement*, Dover Publications, Inc. 1956.
- [3] L. Bachlier, “Théorie de la spéculation” (Paris Doctoral Dissertation in Mathematics, March 29, 1900) *Annales de l’Ecole Normale Supérieure*, ser. 3, XVII (1900), 21-86; “Théorie mathématique du jeu,” *Annales de l’Ecole Normale Supérieure*, ser. 3, XVIII (1901), 143-210; *Calcul des probabilités* (Paris: Gauthier-Villars, 1912); *Le jeu, la chance et le hasard* (Paris, 1914 [reprinted up to 1929 at least]). See also e.g. M. F. M. Osborne, *Operations Research*, VII (1959), 145. The modern authors have suggested that the original assumption of independent increment of $z(t)$ be replaced by the assumption of independent and Gaussian increments of $\ln z(t)$.
- [4] See e.g. B. B. Mandelbrot, *Fractals and Scaling in Finance* (Springer, 1997); and the references given therein.
- [5] B. B. Mandelbrot, *The Journal of Business*, **36**, 394 (1963).
- [6] B. B. Mandelbrot, *The Journal of Business*, **40**, 393 (1967).
- [7] JACEE-Collaboration: T. H. Burnett et al., *Phys. Rev. Lett.* **50**, 2062 (1983).
- [8] NA22-Collaboration: M. Adannis et al. *Phys. Lett.* **B 85** 200 (1987).
- [9] E. A. De Wolf, I. M. Dremin and W. Kittel, *Phys. Reports*, **270** (1 & 2) 1 1996 and the references given therein.
- [10] See e.g. R. E. Marshak, *Conceptual Foundations of Modern Particle Physics*, World Scientific, 1993, p. 284.
- [11] See e.g. A. Messiah, (translated by G. M. Thmmer) *Quantum Mechanics*, Vol **I.** , North-

- Holland Publishing Company, Amsterdam (1967).
- [12] See e.g. P. W. Atkins and R. S. Friedman, *Molecular Quantum Mechanics*, Oxford University Press (1996) p. 25; and the references given therein.
- [13] F. Takagi, Phys. Rev. Lett. **53**, 427 (1984).
- [14] A. Bialas and R. Peschanski, Nucl. Phys. **B** 273, 703 (1986).
- [15] The definitions and theorems (including their proofs) can be found in monographs and text books on Probability Theory and Mathematical Statistics. See e.g.:
- W. Feller, *An Introduction to Probability Theory and Its Applications*, Vol. **I**, **II**, John Wiley & Sons (1971);
- V. V. Uchaikin and V. M. Zolotarev, *Chance and Stability: Stable Distributions and their Applications*, Utrecht, The Netherlands (1999);
- J. P. Nolan, *Stable Distributions Models for Heavy Tailed Data*,
<http://academic2.american.edu/~jpnolan/home.html>;
- WEI Zongshu, *Gailülun Yu Shuli Tongji Jiaocheng (Probability Theory and Mathematical Statistics)*, Gaodeng Jiaoyu Chubanshe, Beijing, China (1983);
- MA Zhenhua et al., *Xiandai Yingyong Shuxue Shouce: Gailü Tongji Yu Suiji Guocheng Juan (Handbook in Modern Applied Mathematics: Probability, Statistics and Random Processes Volume)*, Qinghua Daxue Chubanshe, Beijing, China (2000).

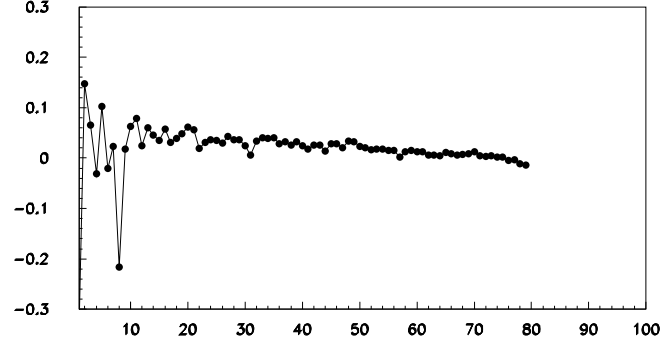


FIG. 1: Running sample mean $\bar{L}_n(\Delta\eta)$ of the $L(\eta, \Delta\eta)$'s [see Eq. (12)] for $\Delta\eta = 0.1$ (the experimental resolution) is plotted as function of the ordering number n . Data are taken from JACEE1 [7]. Here, $\eta_{min} = -4.0$ is the starting point for the ordering of the 80 $\Delta\eta$ -bins. The solid line indicates the ideal case in which $\bar{L}_n \equiv 0$.

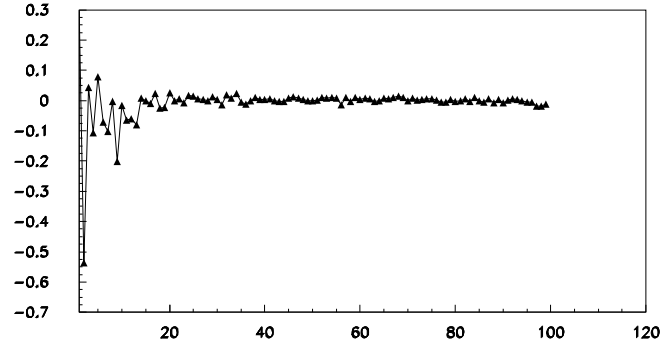


FIG. 2: Running sample mean $\bar{L}_n(\Delta\eta)$ of the $L(\eta, \Delta\eta)$'s for $\Delta\eta = 0.1$ (the experimental resolution) is plotted as function of n . Data are taken from JACEE2 [7]. Here, $\eta_{min} = -5.0$ and there are 100 $\Delta\eta$ -bins. The solid line indicates the ideal case in which $\bar{L}_n \equiv 0$.

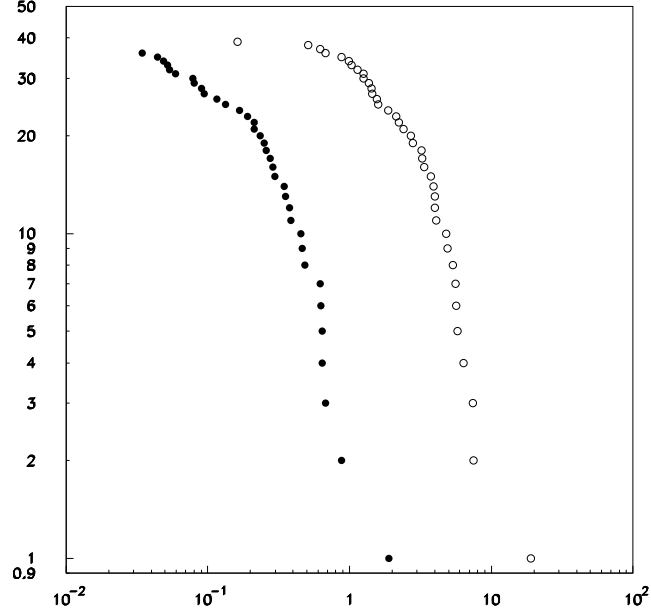


FIG. 3: Tail-distributions of the $L(\eta, \Delta\eta)$'s for JACEE1 [7]: The right-tail distribution $P(L > L^+)$ is shown as a set of black dots. $P(L > |L^-|)$ which is the mirror image of the left-tail distribution $P(L < L^-)$ is shown as a set of open circles. They are plotted as functions of L^+ and $|L^-|$ respectively. Here, $P(L > |L^-|)$ is plotted instead of $P(L < L^-)$ in order to avoid the problem of taking logarithm of negative values; the values of $|L^-|$ are multiplied by a factor 10 so that the two sets of points can be kept away from one another in the figure. This technique used in plotting $P(L < L^-)$ and comparing it with the corresponding $P(L > L^+)$ in the same figure is used throughout the paper whenever it is needed.

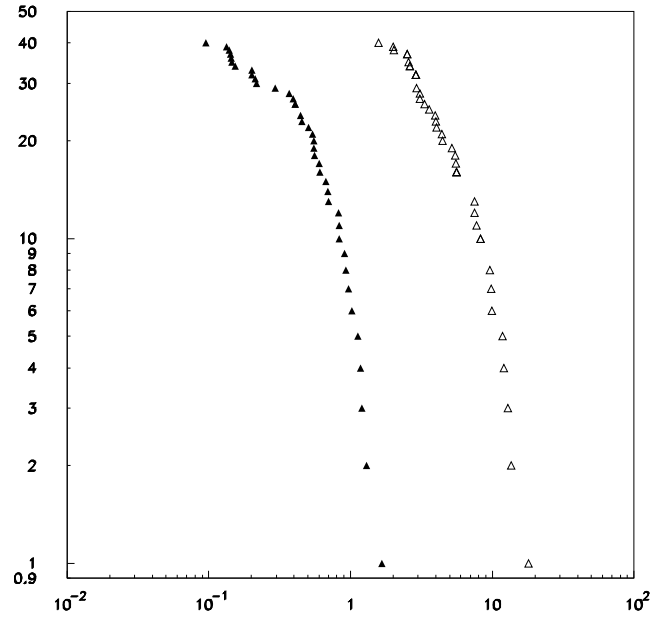


FIG. 4: Tail-distributions of the $L(\eta, \Delta\eta)$'s for JACEE2 [7]: Here the right-tail distribution is shown as a set of black triangles; while those for the left-tail are shown as open triangles. The technique used in plotting $P(L < L^-)$ used here are the same as that used in Fig. 3.

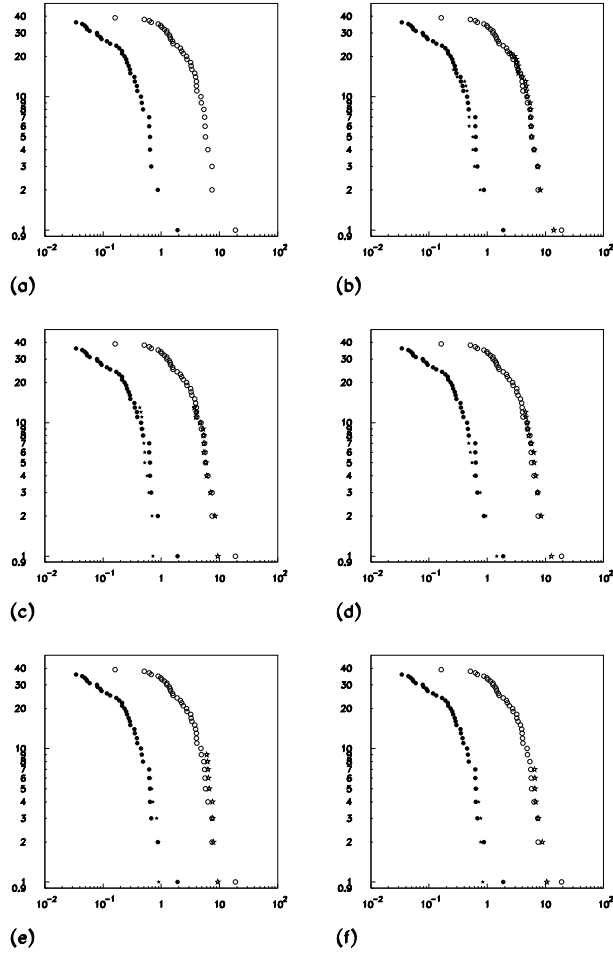


FIG. 5: Direct stability tests for JACEE1 [7]: Figs. 5(b) to 5(f) correspond respectively to the $m = 2, 3, \dots, 6$ cases mentioned in Section IV Step (iii). Here, m stands for the number in equal-size-divided samples in the set of $L(\eta, \Delta\eta)$'s. This is obviously the same m as that in Eq. (14) which expresses the necessary and sufficient condition of stability for the $L(\eta, \Delta\eta)$'s under consideration. The black dots and open circles in all these figures are respectively the right-tail (r-t) and left-tail (l-t) distributions $P(L > L^+)$ and $P(L > |L^-|)$ as functions of L^+ and $|L^-|$. In the figures 5(a) through 5(f) we write simply r-t or l-t as functions of L^+ and $|L^-|$ in order to safe space. They are to be compared separately with the black stars and the open stars which stand respectively for $P(c_m^{-1}[S_m - \gamma_m] > c_m^{-1}[S_m - \gamma_m]^+)$ and $P(c_m^{-1}[S_m - \gamma_m] > |c_m^{-1}[S_m - \gamma_m]^-|)$ for $m = 2, 3, \dots, 6$. In the figures we write simply r-t or l-t as functions of $N_m^+ \equiv c_m^{-1}[S_m - \gamma_m]^+$ or $|N^-| \equiv |c_m^{-1}[S_m - \gamma_m]^-|$ to safe space. Note that the quality of stability can be judged by the degree how good the black stars/open stars overlap with the corresponding black dots/open circles. Fig. 5(a) is a reproduction of Fig. 3 in the same scale as Figs. 5(b) to 5(f), so that comparison in globe view can be made.

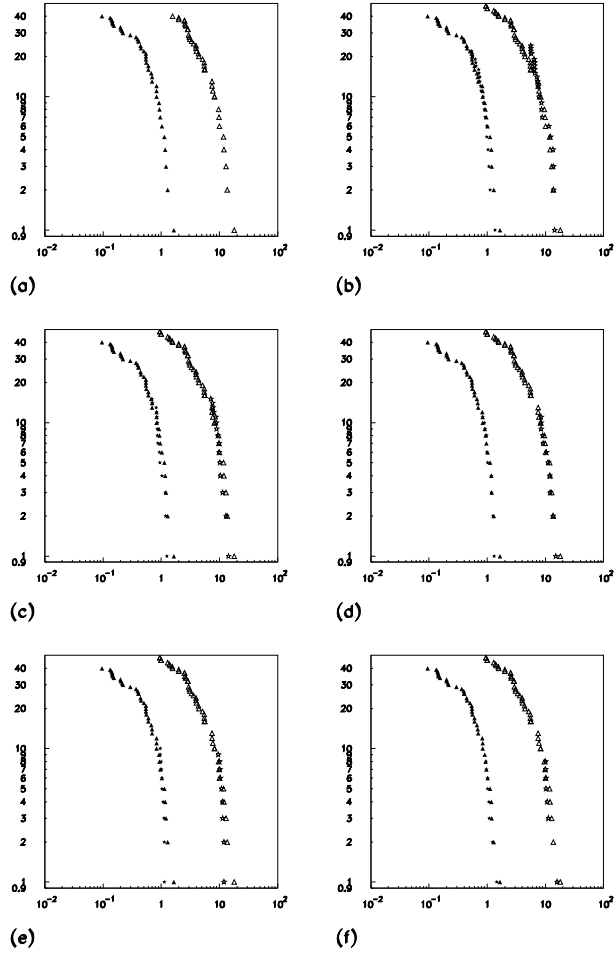


FIG. 6: Direct stability tests for JACEE2 [7]: The notations and the technique in plotting the tail-distributions used here are the same as those used in Fig. 5, except that the black and open circles should now be replaced by black and open triangles.

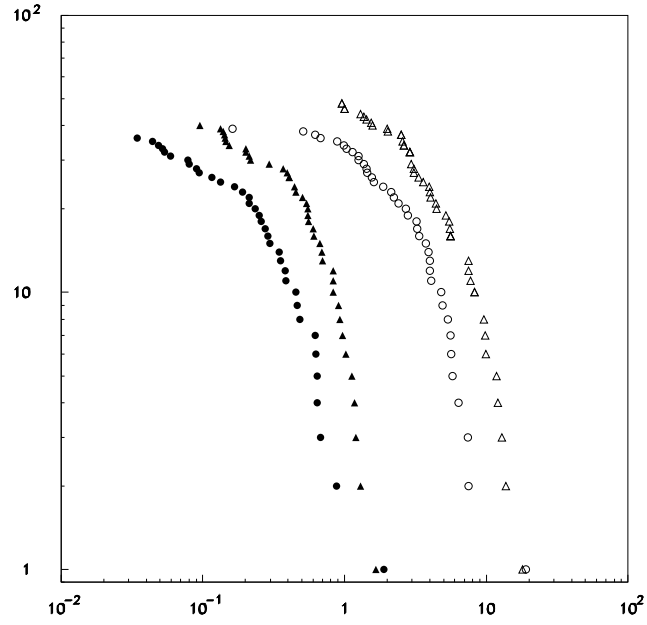


FIG. 7: Stationarity test: The right-tail (r-t) distribution $P(L > L^+)$ and the left-tail (l-t) distribution $P(L > |L^-|)$ for JACEE1 (abbreviated as J1 in the figure) [7] are plotted in the same figure with those for JACEE2 (abbreviated as J2 in the figure) [7]. The JACEE1 data are shown as black dots and open circles respectively, while the corresponding JACEE2 data are shown as black and open triangles.

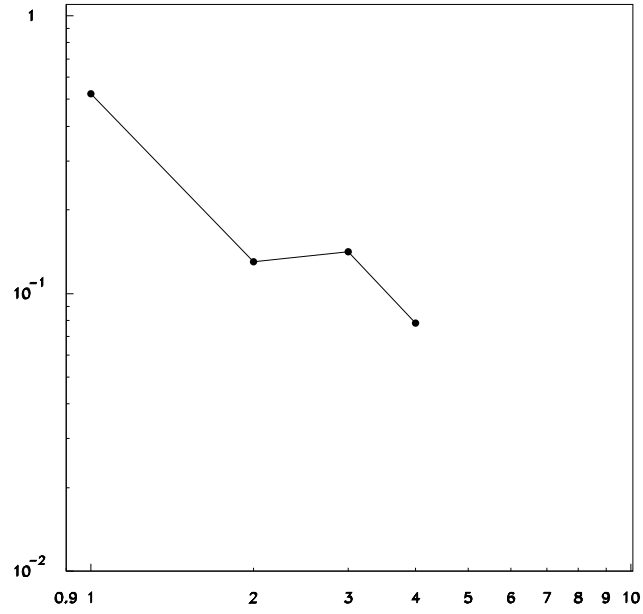


FIG. 8: The variance of samples of the same size (20), $S_{20}^2(\Delta\eta = 0.1)$, is plotted as function of the ordering number m for the $L(\eta, \Delta\eta)$'s obtained from JACEE1 [7]. Due to the limited number of data, $m=1, 2, 3$ or 4 . This figure is the analogue of Fig. 1 of Ref. [6].

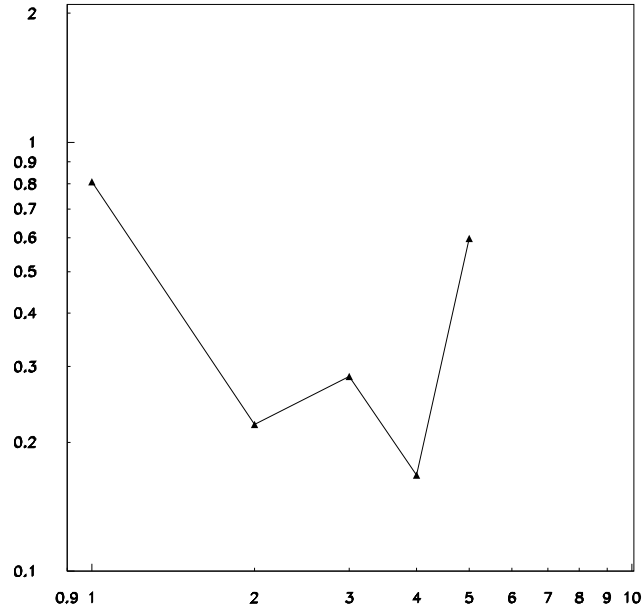


FIG. 9: $S_{20}^2(\Delta\eta = 0.1)$ is plotted against m . Data are taken from JACEE2 [7]. Here, $m=1, 2, 3, 4$ or 5. Also this figure is the analogue of Fig. 1 of Ref. [6].

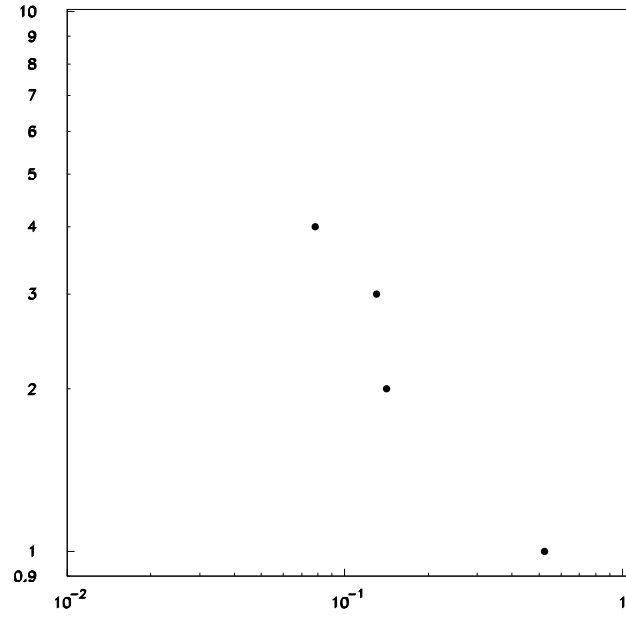


FIG. 10: Scaling test for JACEE1 [7] by using the method proposed by Mandelbrot [6]: This is the cumulated absolute frequency distribution for the S_{20}^2 's shown in Fig. 8. This figure is the analogue of Fig. 2 of Ref. [6].

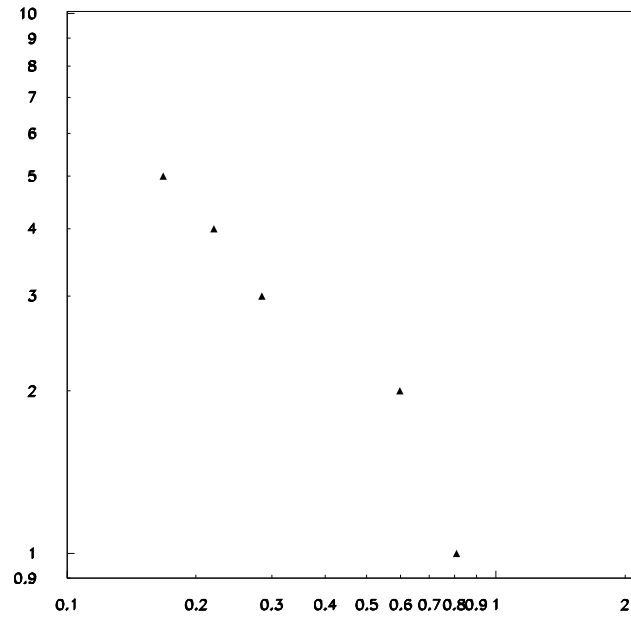


FIG. 11: Scaling test for JACEE2 [7] by using the method proposed by Mandelbrot [6]: This is the cumulated absolute frequency distribution for the S_{20}^2 's shown in Fig. 9. Also this is the analogue of Fig. 2 of Ref. [6].

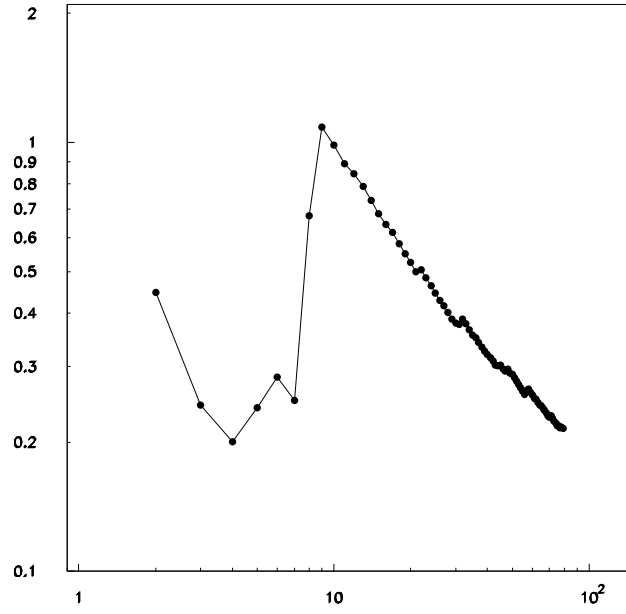


FIG. 12: The running sample variance $S_n^2(\Delta\eta = 0.1)$ for the $L(\eta, \Delta\eta)$'s obtained from JACEE1 [7] is plotted as function of the ordering number n , where $n = 2, 3, \dots, 79$.

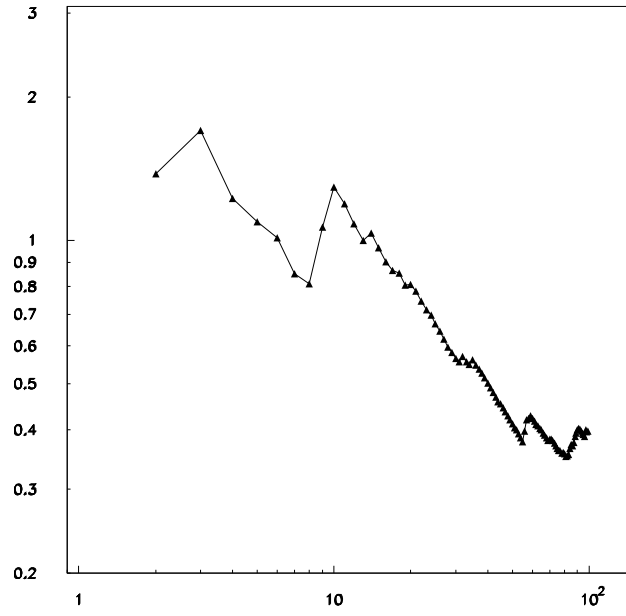


FIG. 13: The running sample variance $S_n^2(\Delta\eta = 0.1)$ is plotted against n . Data are taken from JACEE2 [7], where $n = 2, 3, \dots, 99$.

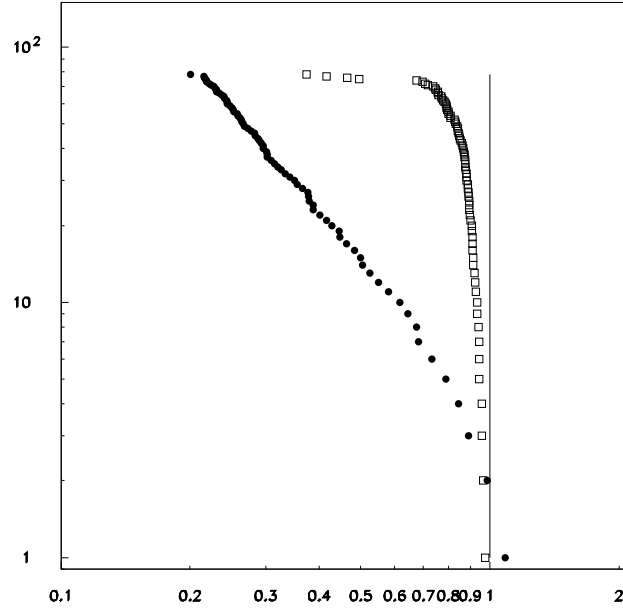


FIG. 14: Scaling test for JACEE1 [7] by using the method proposed in the present paper: The cumulated absolute frequency distribution for the S_n^2 's (calculated and plotted in Fig. 12) is shown as black dots in this figure. For the sake of comparison, a sample of the same size (79 for JACEE1) of standard Gaussian random variables (with zero population mean and unity population variance, $\sigma^2 = 1$) is also taken into account, where the running sample variance S_n^2 's are also calculated, and the corresponding cumulated absolute frequency distribution (denoted by open squares) is plotted. The solid line stands for the mean of S_n^2 of the sample of standard Gaussian random variables for all n 's, that is for $E(S_n^2) = \sigma^2 = 1$. It also stands for the limiting value of the sample variance, which is according to the Law of Large Numbers: $S_n^2 \xrightarrow{P} \sigma^2 = 1$.

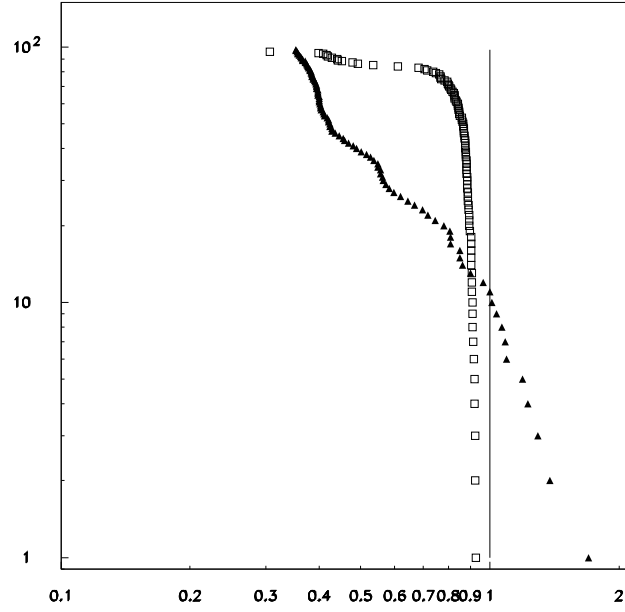


FIG. 15: Scaling test for JACEE2 [7] by using the method proposed in the present paper: The cumulated absolute frequency for the S_n^2 's (calculated and plotted in Fig. 13) is shown as black triangles in this figure. The notations used here are the same as those used in Fig. 14. The size of the JACEE2 sample and that of the corresponding Gaussian sample is 99.